

# Effect of Roughened Surface on Local heat Transfer Distribution Due to Impinging of Circular Synthetic Air Jet

Ravindra Kondaguli<sup>1</sup>, Dr.Omprakash Hebbal<sup>2</sup>, Prof S B Koulagi<sup>3</sup>

<sup>1</sup>M.Tech Scholar Department of Mechanical Engineering PDACE Gulbarga/Karnataka/India

<sup>2</sup>Dr.Omprakash Hebbal Department of Mechanical Engineering PDACE Gulbarga/Karnataka/India

<sup>3</sup>Prof.S B Koulagi Department of Mechanical Engineering BLDE CET Bijapur/Karnataka/India

## Abstract

Air jets have been widely used in many industrial applications in order to achieve enhanced coefficients for convective heating, cooling or drying. A synthetic jet is synthesized directly from the fluid in the system in which it is embedded. A synthetic jet is commonly formed when the fluid is alternately sucked into and ejected from a small cavity by the motion of a diaphragm bounding the cavity. The present work is the study of effect of roughened surface on local heat transfer coefficients. The data with roughened surface is compared with available data of smooth surface. Experiments are conducted for different orifice plate diameter of 6mm 8mm and 10mm. Detached rib if used for roughening the surface detachment distance diameter of the ribs are varied. Heat transfer data for rough surface is compared with data available for smooth surface [22]. It is observed that local heat transfer coefficients are increased significantly in the stagnation region. Electromagnetic actuator is used to produce synthetic jet. Frequency of actuator distance from target plate to orifice plate is varied. Image is captured using Infrared camera

**Keywords:** synthetic jet, electronic cooling, roughened surface,

## 1. Introduction

In the fast growing technology, due to faster operation of each transistor and an increase in their density on integrated circuits, a large amount of heat needs to be dissipated. Thermal overstressing is one of the major causes of failure of electronic components. This underscores the requirement for proper thermal management which is perhaps the most crucial part of the electronic system design. Effective cooling systems are therefore required which also meet the space and other design constraints. Heat sinks with air as the working fluid, and different fin geometry and fan arrays have been traditionally used for heat removal from electronic systems. Due to low cost, availability and reliability, air will continue to be used as the working fluid. In the present work, synthetic jet impingement cooling is considered which can potentially be used for cooling of hot-spots. The interaction of synthetic jets with an external flow near the flow boundary can lead to the formation of

closed recirculation flow regions and consequently to an apparent modification of the flow boundary. This attribute enables synthetic jets to effect significant global modifications of the base flow on scales that are one to two orders of magnitude larger than the characteristic length scales of the jets themselves. Besides cooling, the synthetic jets have a number of other potential engineering applications, such as boundary-layer separation control, jet vectoring, better mixing of fuel in the engine combustion chamber, creation of local turbulence, and vehicle propulsion.

## 2. Experimental Set up

Experimental set up (Fig. 1(a)) basically consists of a synthetic jet generator, heater plate, Stabilized DC power supply, voltage and current measuring devices, infra-red thermal imager, thermocouple, Rib and orifice plate.

The synthetic generator is mounted on a swiveling 2D traversing table and can be fixed at any required distance ( $z$ ) from the target plate. The experiments are conducted for different configurations of circular synthetic jet impinging on a heated surface. A calibrated K type thermocouple is inserted into the synthetic generator cavity in order to measure the jet temperature. Sufficient care is taken so that only thermocouple junction is protruding inside the cylinder and flow is not disturbed much. The target plate assembly is mounted separately on independent 2D traversing tables and aligned so that the jet issued from the orifice impinges the center of the target plate normally. The input voltage to the actuator is maintained constant (3.6V) and the frequency of excitation is controlled by a signal generator and monitored by using an knob present in sine/signal generator.

Power is supplied to the target plate from Ap-lab make CBPS 5/120 type regulated DC power source. The power can be varied through multi-turn voltage setting knob. Four and half digit voltmeter and ammeters give accurate measurements. Suitable voltage taps are provided on the

target plate and connected to high resolution voltmeter. The camera is positioned on the side of the heater opposite to the impinging jet. Thermal imager is positioned on the same table as that of target plate in order to get a perfect view of the zone of action.

A curve fit to the distribution for temperature differences

For  $h_{loss}$  from 8°C to 57°C is

$$h_{loss(eff)} = 4.893(T_w - T_{inf})^{0.341}$$

The other observations of the experiments are shown in the following table.

**Table Observation table :**

Ratio of axial distance and orifice dia (z/d)	Image number	Current to target plate I(Amp)	Voltage across tapping ( $V_{tap}$ )	Ambient temp $T_{amb}$ (°C)	Jet temp reading (in terms of emf) (mV)

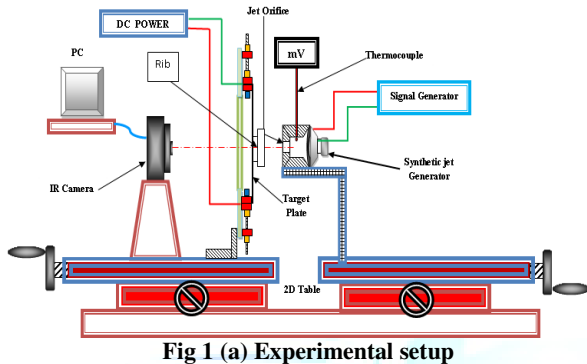


**Fig 1 (a) Experimental setup**

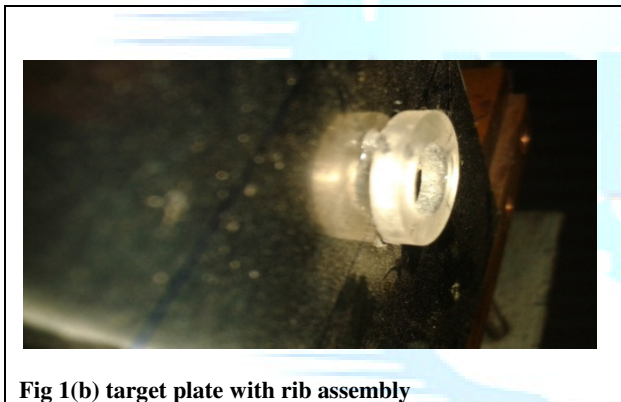


**Fig 1(b) target plate with rib assembly**

### 3 Experimental Methods

**Infra-red thermal imager:** In the present work Infra –red thermal imager of FLUKE make Model FLK-TI 55 FT is used.

- Smart view, together with the thermal imager, enables to:
- (a) Transfer thermo-graphic images to a computer and manage them
  - (b) Optimize and analyze the infrared and visible light control images
  - (c) Create and print detailed, professional reports containing important image data

**3.1 Estimation of Heat loss from target surface:** Heat loss from the exposed surface of the target plate due to natural convection and radiation is estimated experimentally.

The energy balance on the target surface during jet impingement is as given below,  
 Energy supplied as Ohmic dissipation = Energy convected by impinging jet from the front surface + Energy lost

The fig shows the heat loss experiment:

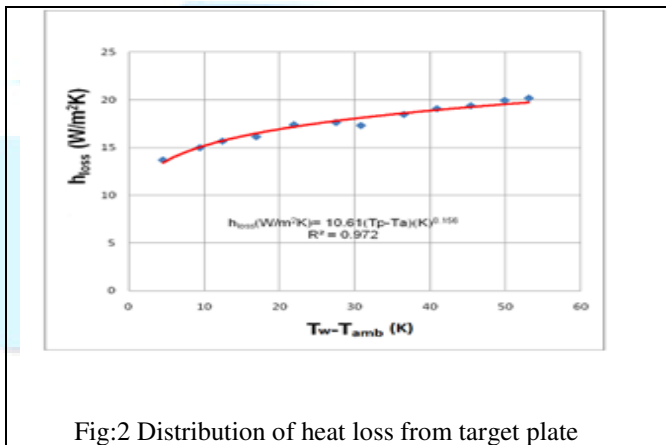
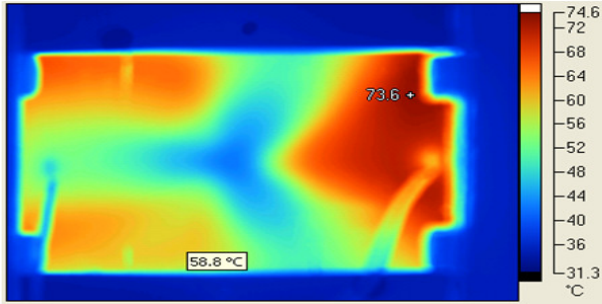


**Fig:2 Distribution of heat loss from target plate**

**Thermal Image:** Thermal Image obtained from IR camera  
 Fig:3 Thermal image



Due to spacer in the stagnation region heat transfer is less in positive radial direction

### 3.2 Data reduction:

Determination of heat transfer co-efficient for heat loss:

$$h_{loss} = \frac{Q_{conv}}{A \times (T_w - T_{amb})}$$

We have,  $Q_{loss}$ , the heat flux imposed on one side of the surface and is calculated as,

$$Q_{loss} = [Q_{rad} + (0.5 \times Q_{conv})]$$

$Q_{rad}$  is the heat lost due to radiation and is given as,

$$Q_{rad} = Q_{rad_b} + Q_{rad_f}$$

where  $Q_{rad_b}$  and  $Q_{rad_f}$  are the heat lost due to radiation from back side and front side of the target plate and are calculated as:

$$Q_{rad_b} = \sigma \epsilon_b (T_w^4 - T_{amb}^4)$$

$$Q_{rad_f} = \sigma \epsilon_f (T_p^4 - T_a^4)$$

and  $Q_{conv}$  is the heat convected to surroundings given as,

$$Q_{conv} = Q_{rad} - Q_{loss}$$

Determination of local Heat transfer co-efficient for impinging jet

$$h = \frac{q_{net}}{T_w - T_j}$$

where  $q_{net}$  is the net heat flux supplied to the target plate

$$q_{net} = q_{joule} - q_{loss}$$

$q_{joule}$  heat flux supplied and is calculated as

$$q_{joule} = \frac{VI}{A}$$

and  $q_{loss}$  is the heat lost and is calculated as

$$q_{loss} = h_{loss}(T_w - T_{amb})$$

$h_{loss}$  is the heat transfer co-efficient for heat loss and is calculated from the equation obtained from heat loss experiment (Section 3.1)

Therefore effective heat transfer co-efficient is given by

$$h_{eff} = 4.893(T_w - T_{amb})^{0.341}$$

## 4 Result and conclusion:

Experiments are conducted for local heat transfer distribution with impinging synthetic jet on flat rough surface at various frequencies, ( $z$  jet to plate distance  $d$ ) considered in the present experimentation varies from 01-12. All experiments are conducted for different orifice diameters. Different dimensioned ribs are used internal diameter of rib is 10mm different external diameter of rib (14mm and 17mm). The other parameter considered here are detachment distances  $Z$  (2mm and 1mm).

### 4 Effect of Roughened surface on stagnation heat transfer coefficient:

#### 4.1 For 6mm Orifice plate:

Fig 4 shows the stagnation heat transfer coefficients for different  $z/d$  on smooth surface without rib where  $d$  is diameter of orifice plate  $z$  is distance from orifice plate to target plate. It is observed that heat transfer coefficients are higher for frequency of 160 Hz and  $z/d=6$ . The Fig 5 shows the stagnation heat transfer coefficient with detached rib of internal diameter 10mm and external diameter of 14mm and detachment of 2mm. It is observed that. From Fig. 5 It is observed that there is increase in stagnation heat transfer coefficient at a frequency of 100Hz and  $z/d=2$  stagnation heat transfer coefficient has increased from 132w/m<sup>2</sup>k without rib to 186w/m<sup>2</sup>k which is nearly 40% increase. It observed that heat transfer coefficients have decreased as  $z/d$  increases. From Fig. 6 It is observed that there is increase in stagnation heat transfer coefficient at a frequency of 140Hz and  $z/d=2$  stagnation heat transfer coefficient has increased from 132w/m<sup>2</sup>k without rib to 175w/m<sup>2</sup>k which is 33% increase. It observed that heat transfer coefficients have decreased as  $z/d$  increases

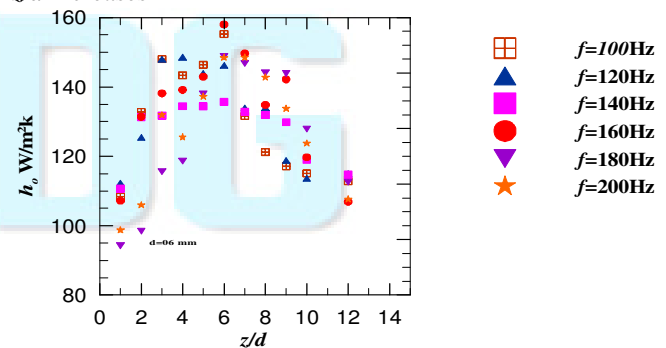


Fig. 4. Stagnation point heat transfer distribution at different frequency and  $z/d$  with  $L/d=1$  for orifice diameter of 6 mm [22]

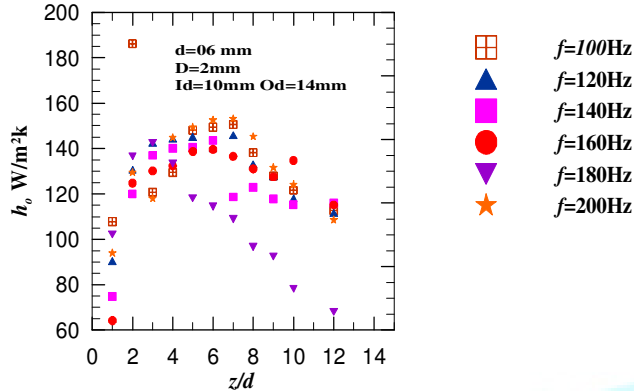


Fig. 5. Stagnation point heat transfer distribution at different frequency and  $z/d$  for orifice diameter of 6 mm rib  $I_d=10\text{mm}$   $O_d=14\text{mm}$  Detachment  $Z=2\text{mm}$

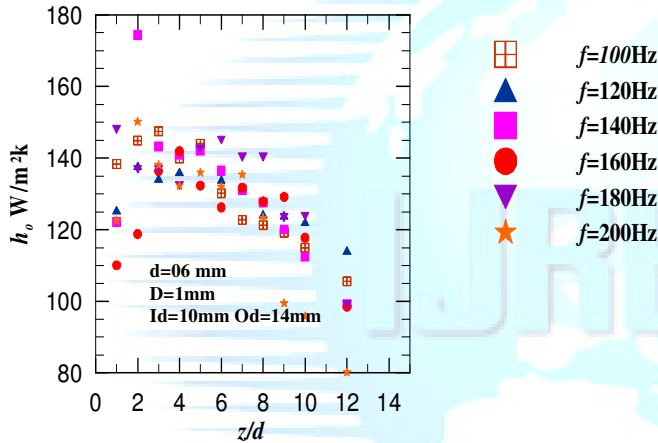


Fig.6. Stagnation point heat transfer distribution at different frequency and  $z/d$  for orifice diameter of 6 mm rib  $I_d=10\text{mm}$   $O_d=14\text{mm}$  Detachment  $Z=1\text{mm}$

**4.2 For diameter of 10mm:**

Fig 7 shows the stagnation heat transfer coefficients for different  $z/d$  on smooth surface without rib. From Fig. 8 It is observed that stagnation heat transfer coefficient is higher at a frequency of 140Hz and  $z/d=5$ . Stagnation heat transfer coefficient has increased from 140w/m<sup>2</sup>k Fig 7 without rib to 160w/m<sup>2</sup>k Fig 8 with rib which is 14.2% increase. It observed that heat transfer coefficients have decreased as  $z/d$  increases further. From Fig.9 It is observed that stagnation heat transfer coefficient is higher at a frequency of 120Hz and  $z/d=5$  stagnation heat transfer coefficient has increased from 135w/m<sup>2</sup>k Fig 7 without rib to 146w/m<sup>2</sup>k Fig. 9 which is 14.8% increase. It observed that heat transfer coefficients have decreased as  $z/d$  increases further.

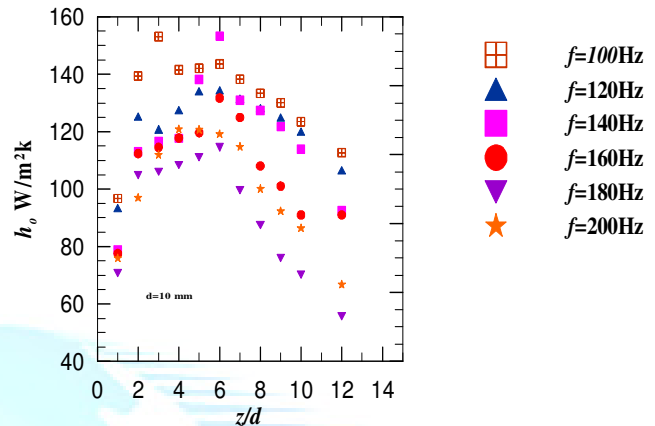


Fig. 7. Stagnation point heat transfer distribution at different frequency and  $z/d$  with  $L/d=1$  for orifice diameter of 10 mm [22]

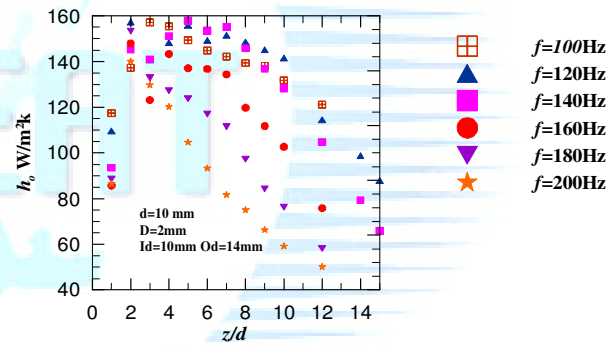


Fig. 8. Stagnation point heat transfer distribution at different frequency and  $z/d$  for orifice diameter of 10 mm rib  $I_d=10\text{mm}$   $O_d=14\text{mm}$  Detachment  $Z=2\text{mm}$

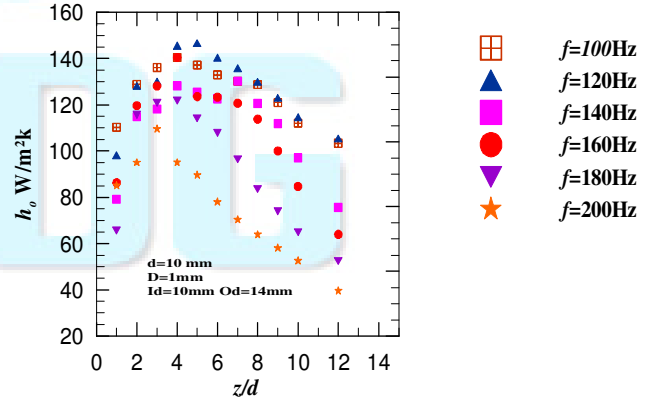


Fig. 9. Stagnation point heat transfer distribution at different frequency and  $z/d$  for orifice diameter of 10 mm rib  $I_d=10\text{mm}$   $O_d=14\text{mm}$  Detachment  $Z=1\text{mm}$

**4.3 For 8mm orifice plate diameter:**

From Fig. 10 It is observed that stagnation heat transfer coefficient is higher at a frequency of 100Hz and  $z/d=4$  stagnation heat transfer coefficient has increased from 145w/m<sup>2</sup>k Fig 10 without rib to 155w/m<sup>2</sup>k Fig 11 which is 14.2% increase. It observed that heat transfer coefficients have decreased as  $z/d$  increases further. From Fig.12 It is observed that stagnation heat transfer coefficient is higher at a frequency of 100Hz and  $z/d=2$  stagnation heat transfer coefficient has increased from 140w/m<sup>2</sup>k Fig10 without rib to 160w/m<sup>2</sup>k Fig 12 which is 14.2% increase. It observed that heat transfer coefficients have decreased as  $z/d$  increases further.

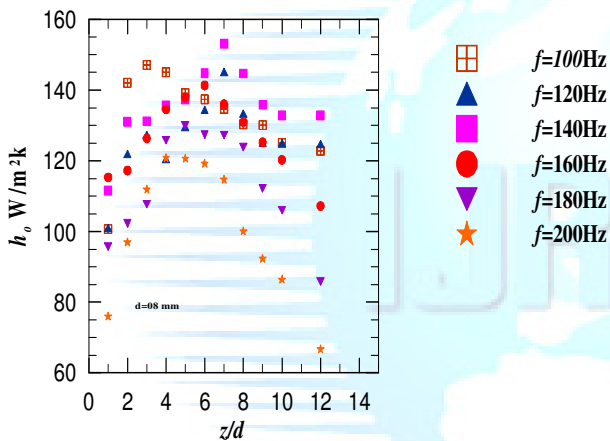


Fig 10. Stagnation point heat transfer distribution at different frequency and  $z/d$  for orifice diameter of 8 mm [22]

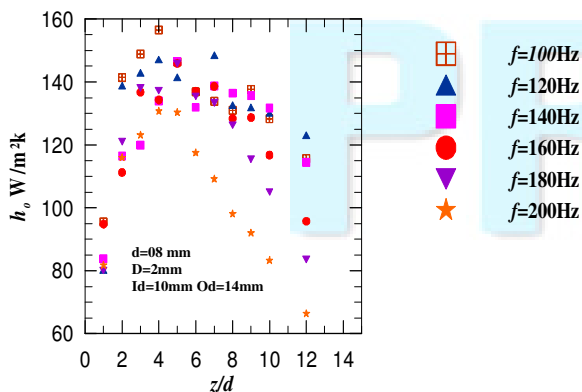


Fig 11. Stagnation point heat transfer distribution at different frequency and  $z/d$  for orifice diameter of 10 mm rib Id=10mm Od=14mm Detachment Z=2mm

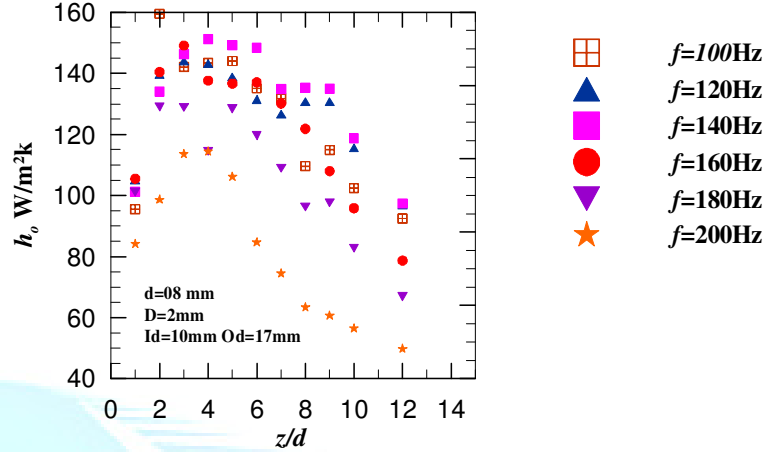


Fig. 12 Stagnation point heat transfer distribution at different frequency and  $z/d$  for orifice diameter of 10 mm rib Id=10mm Od=17mm Detachment Z=2mm

**4.4 Effect of Roughened surface on Local heat transfer coefficient:**

Fig 13 shows radial heat transfer distribution at different  $z/d$   $r$  is radial distance from the stagnation point  $d$  is orifice plate diameter with frequency of 160Hz on smooth surface. Heat transfer coefficients are maximum for  $z/d=6$ . From Fig 14 it is observed that heat transfer coefficients are maximum for  $z/d=2$  secondary peak is observed for positive radial direction due to presence of spacer of rib and heat transfer coefficients are lower in positive radial direction.

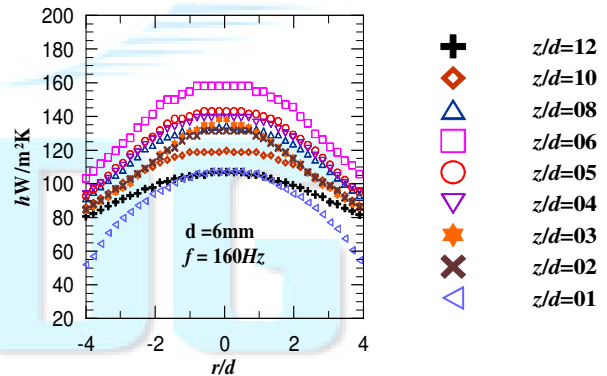


Fig. 13. Radial heat transfer distribution on smooth surface at different  $z/d$  with frequency of 160Hz for orifice diameter of 6 mm [22]

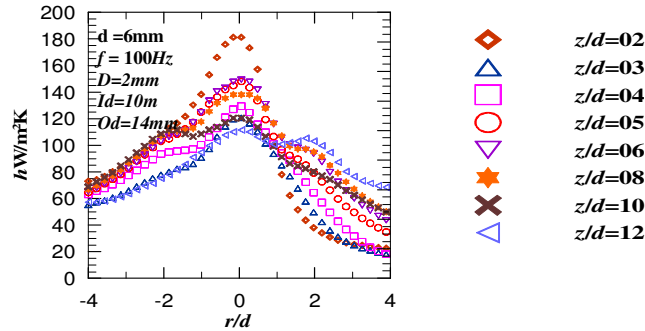


Fig. 14. Radial heat transfer distribution at different  $z/d$  with frequency of 100Hz for orifice diameter of 6 mm Detachment 2mm.rib of ID=10mm OD=14mm

#### 4.5 For 10mm orifice plate

From Fig 15 it is observed that heat transfer coefficients are higher for  $z/d=6$  for smooth surface. From Fig 16it is observed that heat transfer coefficients are higher for  $z/d=5$  and a secondary peak is observed in positive radial direction due to the presence of spacer in the stagnation line. It is also observed that heat transfer coefficients are higher when compared smooth surface

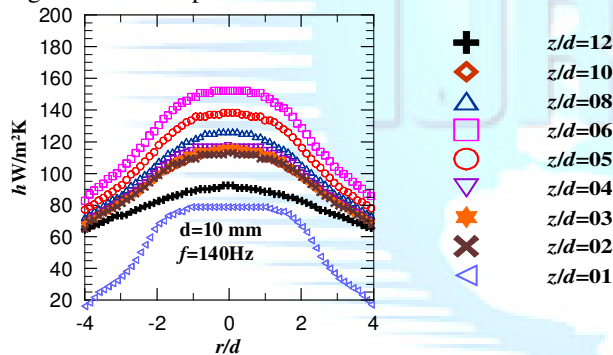


Fig. 15 Radial heat transfer distribution at different  $z/d$  with frequency of 140Hz for orifice diameter of 10 mm[22]

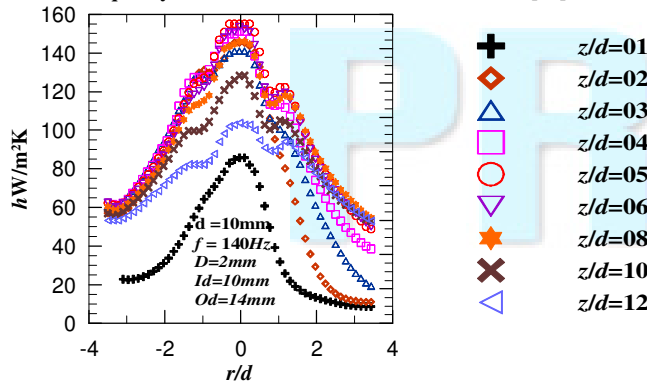


Fig. 16. Radial heat transfer distribution at different  $z/d$  with frequency of 140Hz for orifice diameter of 10 mm

#### Conclusions:

Experiments are conducted for local heat transfer distribution with impinging synthetic jet on flat roughened surface using ribs at various frequencies, jet to plate distance ( $z/d$ ) considered in the present experimentation varies from 1-12. Following are the conclusions of the present work.

- The jet temperature increases above atmospheric temperature at lower jet-to plate distances.
- The local heat transfer coefficients peak at the stagnation point and decrease in radial direction
- For orifice plate having diameter at the orifice 6mm and thickness 6mm stagnation heat transfer coefficients are higher for  $z/d=2$  frequency 100Hz for rib of external diameter 14mm internal diameter 10mm and 2mm detachment there is an 40% increase in stagnation heat transfer coefficient when compared to heat transfer coefficients without rib for same configuration
- For orifice plate having diameter at the orifice 6mm and thickness 6mm stagnation heat transfer coefficients are higher for  $z/d=2$  frequency 140Hz for rib of external diameter 14mm internal diameter 10mm and 1mm detachment there is an 33% increase in stagnation heat transfer coefficient when compared to heat transfer coefficients without rib for same configuration
- For orifice plate having diameter at the orifice 10mm and thickness 10mm stagnation heat transfer coefficients are higher for  $z/d=5$  frequency 140Hz for rib of external diameter 14mm internal diameter 10mm and 2mm detachment there is an 14.2% increase in stagnation heat transfer coefficient when compared to heat transfer coefficients without rib for same configuration
- For orifice plate having diameter at the orifice 8mm and thickness 8mm stagnation heat transfer coefficients are higher for  $z/d=4$  frequency 100Hz for rib of external diameter 14mm internal diameter 10mm and 2mm detachment there is an 14.2% increase in stagnation heat transfer coefficient when compared to heat transfer coefficients without rib for same configuration
- Due to presence of spacer in the positive radial direction a secondary peak is observed due to vortices generated at the spacers
- Heat transfer coefficients are higher up to  $z/d=5$  as  $z/d$  has increased further heat transfer coefficients have reduced

- Heat transfer coefficients have increased up to frequency of 140Hz further heat transfer coefficients have decreased

### REFERENCES

- [1] Nevins, R.G. and Ball, H.D. 1961. Heat Transfer Between a Flat Plate and a Pulsating Impinging Jet. *Proc. of the National Heat Transfer Conference*, Boulder, CO, **60**, pp. 510-516.
- [2] Kataoka, K, Suguro, M., Degawa, H., Maruo, K., and Mihata, I. 1987. The Effect of Surface Renewal Due to Large-scale Eddies on Jet impingement Heat Transfer. *Int. J. Heat Mass. Trans.*, **30**, pp. 559-567.
- [3] Eibeck, P.A., Keller, J.O., Bramlette, T.T., and Sailor, D.J. 1993. Pulse Combustion: Impinging Jet Heat Transfer Enhancement. *Combust. Sci. Tech.*, **94**, pp. 147-165.
- [4] Smith B. L. and Glezer A. “The formation and evolution of synthetic jets” *Physics of fluids* volume 10, Number 9, 1998, pp. 2281-2297
- [5] Sailor, D. J., Rohli, D.J., Fu, Q. 1999. Effect of Variable Duty Cycle Flow Pulsations on Heat Transfer Enhancement for an Impinging Air Jet. *Int. J. Heat and Fluid Flow*, **20**, pp. 574-580.
- [6] Zulkifli, R., Benard, E., Raghunathan, S., and Linton, A. 2004. Effect of Pulse Jet Frequency on Impingement Heat Transfer. AIAA paper 2004-1343.
- [7] Hwang, S.D., Lee, C.H., and Cho, H.H. 2001. Heat Transfer and Flow Structures in Axisymmetric Impinging Jet Controlled by Vortex Pairing. *Int. J. Heat and Fluid Flow*, **22**, pp. 293-300
- [8] Hwang, S.D. and Cho, H.H. 2002. Effects of Acoustic Excitation Positions on Heat Transfer and Flow in Axisymmetric Impinging Jet: main Jet Excitation and Shear layer Excitation. *Int. J. Heat and Fluid Flow*, **24**, pp. 199-209.
- [9] Cater J. E. and Soria J. “The evolution of round zero-net-mass-flux jets” *J. Fluid Mech.* vol. 472, 2002, pp. 167-200.
- [10] Utturkar Y, Arik M., Charles E. S. and Gursoy M. “An Experimental and Computational Heat Transfer Study of Pulsating Jets” *J. of Heat Transfer* , Vol. 130, June 2008 pp.062201-1-10
- [11] Arik M. “An investigation into feasibility of impingement heat transfer and acoustic abatement of meso scale synthetic jets”. *Applied Thermal Engineering* ,27, 2007, 1483–1494
- [12] Haneda, Y., Tsuchiya, Y., Nakabe, K., and Suzuki, K. 1998. *Int. J. Heat and Fluid Flow*, **19**, pp. 115-124.
- [13] Camci, C. and Herr, F. 2002. Forced Convection Heat Transfer Enhancement Using a Self-Oscillating Impinging Planar Jet. *J. Heat Trans.* **124**, pp. 770-782.
- [14] Smith , B.L. and Swift G.W. “A comparison between synthetic jets and continuous jets” *Experiments in Fluids* ,34, 2003, pp.467–472
- [15] Mallinson J.A., Reizes S. G., Hong G. and Westbury P.S. “Analysis of hot-wire anemometry data obtained in a synthetic jet flow”. *Experimental Thermal and Fluid Science* , vol. 28, 2004, pp.265–272
- [16] O'Donovan, T.S., “Fluctuating heat transfer to an impinging air jet,” 2005. Thesis, University of Dublin, Department of Mechanical & Manufacturing Engineering, Trinity College, Dublin 2.
- [17] O'Donovan, T.S., “Fluctuating heat transfer to an impinging air jet,” 2005. Thesis, University of Dublin, Department of Mechanical & Manufacturing Engineering, Trinity College, Dublin 2.
- [18] Chaudhari M., Verma G., Puranik B., and Agrawal A. “Frequency response of a synthetic jet cavity” *Experimental Thermal and Fluid Science*, 33, 2009, pp. 439–448
- [19] Chaudhari M., Puranik B. and , Agrawal A. “Heat transfer characteristics of synthetic jet impingement cooling” *International Journal of Heat and Mass Transfer* , vol.53, 2010, pp. 1057–1069
- [20] Chaudhari M., Puranik B. and Agrawal A. “Effect of orifice shape in synthetic jet based impingement cooling” *Experimental Thermal and Fluid Science* , vol.34, 2010, pp.246–256
- [21] Gopikrishna et al 2010 “An experimental study of radial wall jet formed by the normal impingement of a round synthetic jet “
- [22] Dr.V V KATTI et al “Local heat transfer distribution due to impinging of circular synthetic air jet” International conference on recent advances in engineering sciences MET 29 2014